Molecular dynamics simulation of tethered membranes in four and five dimensions

Sandra J. Barsky and Michael Plischke
Physics Department, Simon Fraser University, Burnaby, British Columbia, Canada V5A 1S6
(Received 6 June 1994)

We have carried out extensive molecular dynamics simulations of self-avoiding tethered membranes embedded in four- and five-dimensional space. These calculations were performed for a wide range of effective hard-core diameters in order to determine whether or not a crumpling transition exists. We find, in agreement with previous work, that self-avoiding tethered membranes are always flat in $d = 4$ and crumpled in $d = 5$.

PACS number(s): 05.70.Fh, 36.20.Ey, 64.60.Fr

I. INTRODUCTION

The tethered membrane model was originally introduced by Kantor, Kardar, and Nelson [1] as a generalization of linear polymers and as a prototype for models of real two-dimensional systems [2]. In its simplest version, a tethered membrane consists of particles that occupy the vertices of a D dimensional lattice (normally $D = 2$) and which fluctuates in d dimensions. In the absence of self-avoidance such membranes are crumpled with a radius of gyration R_g that scales with the linear dimension of the network as $R_g \sim (\ln L)^{1/2}$. In the thermodynamic limit $L \to \infty$, $R_g^d \ll L^2\sigma^d$, where σ is a measure of the diameter of the particles, indicating that self-avoidance will play an important role for any d, in contrast to linear polymers which become ideal above an upper critical dimension $d_{uc} = 4$. Indeed, a large body of numerical work [3–7] has led to the generally accepted conclusion that self-avoiding membranes without compensating long-range attractive forces are flat for the most interesting case $d = 3$ no matter how small the self-avoidance. This is in marked contrast to Flory theory [1] which predicts an isotropically crumpled phase $R_g \sim L^{\nu_F}$ with $\nu_F = (D + 2)/(d + 2)$. An appealing physical argument [6] for the existence of the flat phase is that tethering, together with self-avoidance generates an effective bending rigidity that is large enough to stabilize the flat phase. However, one would expect that by decreasing the hard core diameter [3] or diluting the membrane [7,8] one could decrease this effective bending rigidity sufficiently to induce a transition to the crumpled phase. To date all efforts to attain this crumpled phase for membranes with purely repulsive interactions in $d = 3$ have failed.

While computer simulations for the three-dimensional case seem to be generally consistent, it is still of interest to explore the complete phase diagram of tethered membranes and, in particular, to determine whether or not a crumpling transition occurs in higher dimensions. In this context, there are a number of theoretical predictions based on different approximations. Goulian [9] and Le Doussal [10] have predicted that the flat phase is stable for $d \leq 4$ on the basis of a variational approximation. Guitter and Palmeri [11], on the other hand, have conjectured that $d = 3$ is the upper limit for the existence of the flat phase for the case of long-range repulsive interactions. Le Doussal and Radzihovsky [12] have constructed a self-consistent theory of the flat phase that predicts the transverse roughening exponent ζ in all dimensions as well as a universal negative Poisson ratio independent of the embedding dimension d.

To date, there has been one other simulation of tethered membranes in higher dimension. Grest [13] carried out molecular dynamics calculations for self-avoiding membranes in $d = 4$, 5, 6, and 8. He concluded that self-avoiding membranes are flat in $d = 4$ and crumpled in $d \geq 5$. The tethering potential used in these simulations produces a rather rigid membrane — one that should have a large induced bending rigidity and should therefore favor the flat phase. In our calculations, which are complementary to those of Ref. [13], we have used a less rigid tethering potential and have varied the effective hard-core diameter over a large range in $d = 4$ in an effort to find a crumpled phase. We have also attempted to reduce the effective bending rigidity in a number of other ways. Our results are entirely consistent with those of Ref. [13]. We find no evidence of a crumpled phase in $d = 4$ and no evidence of a flat phase in $d = 5$. Thus it seems that in dimensions in which both fixed points exist, one or the other always has the entire parameter space as its basin of attraction, as predicted by the theories of [9] and [10].

The structure of this paper is as follows. In Sec. II we describe the model that we have used and the simulations. Section III contains the results of the calculations and we conclude in Sec. IV with a brief discussion.

II. MODEL AND COMPUTATIONAL METHOD

The membranes that we simulated consisted of hexagonal sections of a triangular lattice [14]. The number of particles, N, is related to the longest diameter of the hexagon, L, through $N = (3L^2+1)/4$. Nearest neighbors are tethered to each other by the attractive potential

$$V_{nn}(r_{ij}) = -0.5kR_0^2 \ln(1 - r_{ij}^2/R_0^2) \tag{2.1}$$

and self-avoidance is imposed by the repulsive potential

$$V(r_{ij}) = 4\epsilon \left[\left(\frac{\sigma}{r_{ij}} \right)^{12} - \left(\frac{\sigma}{r_{ij}} \right)^{6} + \frac{1}{4} \right] \tag{2.2}$$

for $0 < r_{ij} \leq 2^{1/6}\sigma$. The potential (2.2) acts between any pair of particles for a fully self-avoiding membrane. In most of the calculations we have taken $k\sigma_0^2/\epsilon = 4$, where the reference length $\sigma_0 = 1$ defines the basic unit of length. We have also typically taken $R_0 = 4.0\sigma_0$ and fixed the average temperature at $k_BT/\epsilon = 1$. The effective hard-core diameter σ is a variable parameter that controls the degree of self-avoidance with $\sigma = 0$ corresponding to a phantom network. In our four-dimensional simulations, we varied σ over the range $0.1 \leq \sigma \leq 1$. For this range of σ, the ratio of turning points r_{min}/r_{max} for a nearest neighbor pair, with average kinetic energy, varies from 0.10 at $\sigma = 0.1$ to 0.66 at $\sigma = 1.0$. In the simulations of Ref. [13], the parameters used were $R_0 = 1.5\sigma_0$, $k\sigma_0^2/\epsilon = 30$, and $\sigma = 1.0$. For these parameters $r_{min}/r_{max} \approx 0.88$, i.e., the membrane is considerably stiffer than any of the ones simulated here.

In the four-dimensional case, we reduced the stiffness and therefore the effective bending rigidity in two other ways. First, we imposed self-avoidance only between particles that are *not* nearest neighbors on the network. This allowed nearest neighbors to interpenetrate and more folding of adjacent triangles. Since this change is purely local, this model should exhibit the same phases in the thermodynamic limit as a fully self-avoiding membrane. Second, we also studied the four-dimensional version of a model of Kantor and Kremer [15]. In this model self-avoidance is imposed only up to a certain maximum distance and, for a fixed such distance, the membrane is phantom in the thermodynamic limit. By studying the behavior of membranes as a function of the cutoff distance one can obtain some insight into whether or not a crumpling transition exists in fully self-avoiding membranes.

Our simulations were constant energy molecular dynamics calculations, with the equations of motion integrated using a standard Verlet algorithm, with a typical time step $\tau = 0.005\sigma\sqrt{m/\epsilon}$. For this value of τ, energy is conserved to better than one part in 10^4 over the duration of a run. These runs were generally at least 2×10^6 time steps long, and the average run was several this length. Every 200 time steps the inertia tensor

$$I_{\alpha\beta} = \frac{1}{N} \sum_i (r_{i\alpha} - \bar{r}_\alpha)(r_{i\beta} - \bar{r}_\beta) \tag{2.3}$$

was diagonalized and the eigenvalues ordered from smallest, λ_1 to largest λ_d. To verify that the samples were well equilibrated and that we had statistically independent data, we calculated autocorrelation functions of these eigenvalues. For the largest membranes simulated, $L = 71$ or $N = 3781$, the relaxation time was roughly 2000 time steps. Thus, even in the worst case, we had several hundred statistically independent configurations.

III. RESULTS

We begin with selected results for fully self-avoiding membranes in $d = 4$. In Fig. 1 we show the eigenvalues λ_j for $\sigma = 1$ and system sizes ranging from $L = 7$ to 71. These are the stiffest of the membranes simulated and the data show quite clearly the anisotropy of these membranes. The two largest eigenvalues can, for large L, be well fitted by the functional form $\lambda_{3,4} \sim L^2$, whereas the two smallest eigenvalues scale with a distinctly smaller exponent: $2\zeta = 2\nu_{1,2} \approx 1.65$ (Fig. 1). These results are entirely consistent with those of Grest [13] who found $\zeta = 0.84 \pm 0.05$ and $\nu_{\|} = \nu_{3,4} = 0.95 \pm 0.05$. We also calculated the Poisson ratio σ_P from fluctuations of the eigenvalues λ_j [16] for $7 \leq L \leq 41$. Over this range of L, the Poisson ratio is almost independent of L and extrapolates to a value of -0.34 at $L^{-1} = 0$, consistent with the prediction of Ref. [12] of a universal negative Poisson ratio in the flat phase of $\sigma_P = -\frac{1}{3}$, independent of embedding dimension.

We also simulated membranes with σ as small as 0.1. The considerable crossover effects for the smaller values of σ are illustrated in Fig. 2 where the eigenvalues are plotted for $\sigma = 0.2$ for $7 \leq L \leq 71$. The clear difference in slope between the straight-line fits to λ_3 and λ_4 and the two smaller eigenvalues is evident. We can quantify this difference by calculating effective exponents

$$\nu_{j,eff}(L_1, L_2) = \frac{1}{2} \frac{\ln\{\lambda_j(L_1)/\lambda_j(L_2)\}}{\ln\{L_1/L_2\}}. \tag{3.1}$$

These exponents are plotted in Fig. 3 as a function of $1/L_1$ where L_1 is the larger of two successive system sizes. Although the data are noisy, it is quite clear that the two larger exponents are essentially equal to each other and will extrapolate to a value close to 1 for $L \to \infty$. The Poisson ratio σ_P is also shown on this plot; again, it extrapolates to a value close to the predicted $\sigma_P = -\frac{1}{3}$ [12].

In Fig. 4 we show the "aspect ratio" $A_1 = \lambda_1/\lambda_4$ as function of σ for various system sizes. The curves drawn through the data points are merely guides to the eye. At $\sigma = 0$, which corresponds to the isotropically crumpled phantom membrane, A_1 increases as function of L, just as in $d = 3$ [4,5]. The points at which the various curves intersect are an indicator of where the crossover from

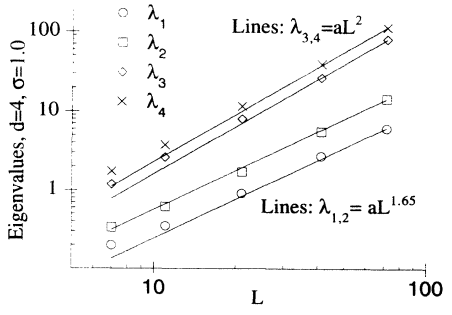

FIG. 1. Eigenvalues of the inertia tensor (2.3) for $\sigma = 1.0$ in $d = 4$. Uncertainties are roughly the size of the data points.

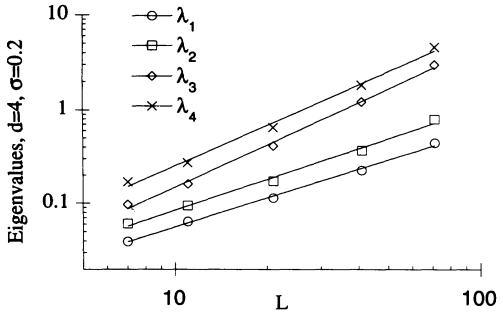

FIG. 2. Eigenvalues of the inertia tensor (2.3) for $\sigma = 0.2$ in $d = 4$. The straight line fits yield exponents $\nu_{3,4} \approx 0.75$ and $\nu_{1,2} \approx 0.5$. Note, however, that there is considerable curvature in the data.

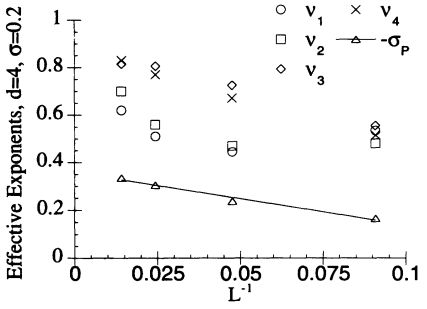

FIG. 3. Effective exponents from (3.1) for the data of Fig. 2 as function of L^{-1}. Also shown is the Poisson ratio σ_P determined from fluctuations of the eigenvalues of the inertia tensor [16] and a straight line fit that indicates an asymptotic value $\sigma_P(\infty) \approx -0.35$.

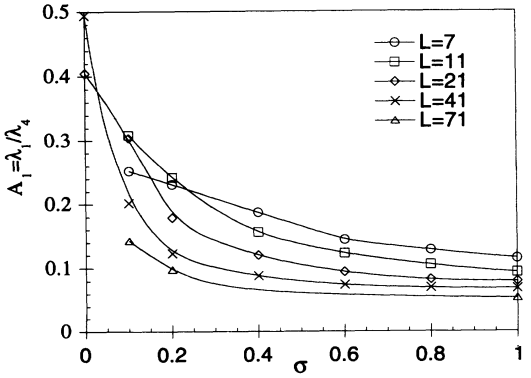

FIG. 4. Plot of the anisotropy $A_1 = \lambda_1/\lambda_4$ as function of σ for various L in $d = 4$.

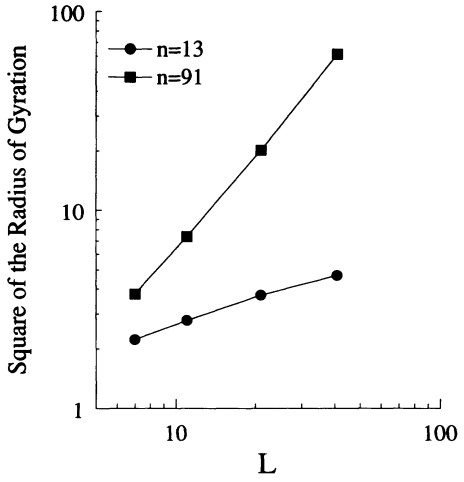

FIG. 5. The radius of gyration of membranes in $d = 4$ with finite-range repulsive interaction. The lower curve is typical of phantom membranes, the upper of self-avoiding membranes.

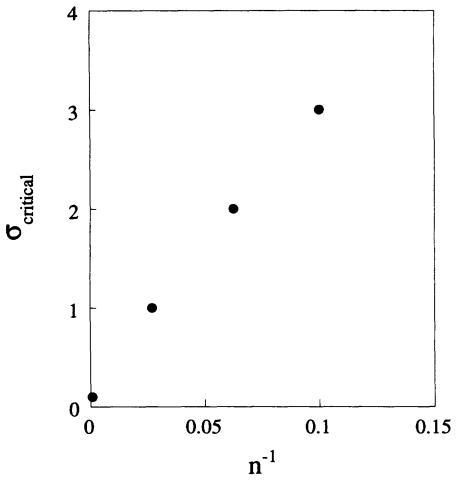

FIG. 6. Estimate of the critical hard-core radius for the transition from crumpled to flat behavior as a function of n^{-1}, where n is a measure of the range of self-avoidance (see text).

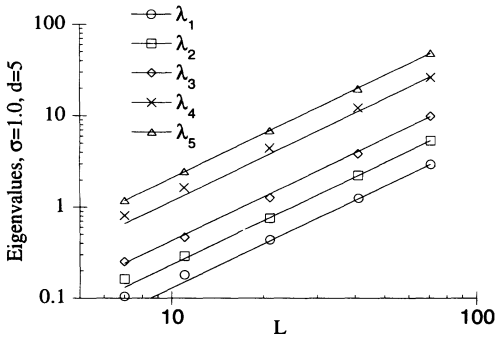

FIG. 7. Eigenvalues of membranes with $\sigma = 1.0$ in $d = 5$ along with fits to the form $\lambda_j = a_j L^{1.60}$.

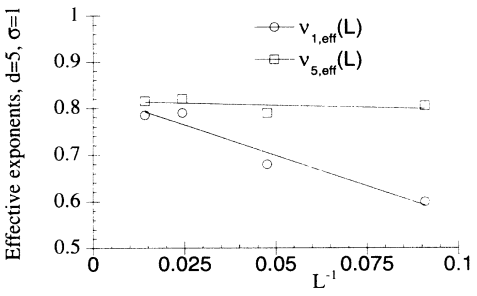

FIG. 8. Effective exponents from (3.1) for the largest and smallest eigenvalues of Fig. 7. The straight line fits yield $\nu_1(\infty) \approx 0.82$, $\nu_5(\infty) \approx 0.83$.

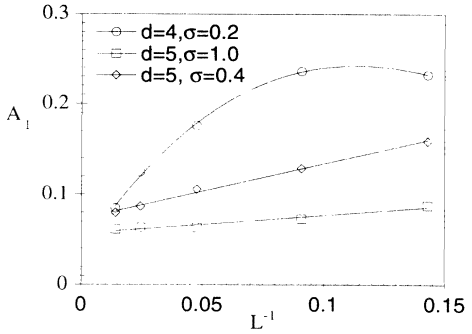

FIG. 9. Anisotropy $A_1 = \lambda_1/\lambda_5$ in $d = 5$ and $A_1 = \lambda_1/\lambda_4$ in $d = 4$ as function of L^{-1}.

crumpled to flat phase takes place.

As mentioned in Sec. II, we also reduced the effective bending rigidity of membranes in $d = 4$ in order to gain more insight into their behavior. In particular, we studied a model of Kantor and Kremer [15] in which self-avoidance is strictly of finite range. In this model, self-avoidance is imposed between a given particle and all other particles within a certain range on the two-dimensional network. This range can be parametrized by the quantity n which denotes the number of particles, including the central particle, that are fully self-avoiding. Thus for $n = 7$ a given particle interacts only with its six nearest neighbors, for $n = 13$ with the two nearest neighbor shells, etc. We carried out simulations for systems of up to size $L = 41$ for $n = 7, 13, 19, 37, 91$ and for $0.025 \leq \sigma/R_0 \leq 0.75$. Clearly, in the thermodynamic limit at fixed n, this model must behave like a phantom membrane and an *ad hoc* criterion is needed to infer the behavior of the system of interest, which is attained when $n \to L$, $L \to \infty$. In Ref. [15] the authors defined an effective "critical diameter" $\sigma_c(n)$ in $d = 3$ by locating a point at which the largest eigenvalue increases sharply when plotted as function of the variable σn^2 and attempted to extrapolate this value of σ to $n = \infty$. We have chosen a different criterion. When n is sufficiently small, compared to the available range of L, the effective scaling exponent of the radius of gyration decreases with increasing system size, consistent with $R_g^2 \sim \ln L$. Conversely, if n is large enough to make the system flat over a range of L, the effective exponent is constant or increases. These two types of behavior are shown in Fig. 5 for the two cases $n = 13$ and 91. We estimated $\sigma_c(n)$ from the value of n at which the effective exponent begins to increase [17]. This function is plotted in Fig. 6 as function of n^{-1}. The data indicate a limiting value of $\sigma_c(\infty) \approx 0$, consistent with the results for fully self-avoiding membranes.

We now turn to the five-dimensional case. We simulated fully self-avoiding membranes for a range of σ and, as in $d = 4$, for $7 \leq L \leq 71$. The behavior of these membranes contrasts sharply with the four-dimensional ones. In Fig. 7 we plot the eigenvalues for $\sigma = 1$, i.e., a rather stiff membrane. There are clear indications of crossover in the three smaller eigenvalues and the straight lines which are fits of the data to the function $\lambda_j = a_j L^{1.6}$ provide a very adequate fit at large L. Further evidence for the conclusion that five-dimensional membranes are isotropically crumpled is presented in Fig. 8 in which the effective exponents (3.1) for the largest and smallest eigenvalues are plotted as function of L^{-1}. The straight line fits have intercepts at $L^{-1} = 0$ of 0.82 and 0.83, respectively. These estimates are consistent with the result $\nu = 0.85 \pm 0.05$ of Ref. [13] and with our own results for different values of σ. Finally, in Fig. 9 we illustrate the striking difference between $d = 4$ and 5 by plotting the aspect ratio $A_1(L) = \lambda_{min}/\lambda_{max}$ as function of L^{-1} for two values of σ in $d = 5$ and for $\sigma = 0.2$ in $d = 4$. It is clear from this figure that $A_1(\infty)$ is finite in $d = 5$ but that it is likely equal to zero in $d = 4$.

IV. CONCLUSION

In this paper, we have reported the results of extensive molecular dynamics simulations of self-avoiding tethered membranes in $d = 4$ and 5. Our main conclusions are that, in any embedding dimension, such membranes are either flat or crumpled in the thermodynamic limit and that in the absence of long-range attraction between the particles on the network there is no crumpling transition. This is consistent with previous numerical work [13] and with some approximate analytical results [9,10]. Our results provide further evidence that the lower critical dimension for the crumpled phase is $4 \leq d_{lc} \leq 5$, which disagrees with the conjecture of Ref. [11] of $d_{lc} = 3$. We have also calculated the Poisson ratio for membranes in $d = 4$ and find that it is generically negative, insensitive to the size of the hard-core diameter and quite close to the universal value predicted by Ref. [12] for membranes in the flat phase.

ACKNOWLEDGMENTS

We thank David Boal, Mark Goulian, Gary Grest, and Emmanuel Guitter for helpful conversations. This research was supported by the NSERC of Canada.

[1] Y. Kantor, M. Kardar, and D. Nelson, Phys. Rev. Lett. **57**, 791 (1986).
[2] For possible realizations of two-dimensional tethered membranes, see, e.g., X. Wen, C. Garland, T. Hwa, M. Kardar, E. Kokufuta, Y. Li, M. Orkisz, and T. Tanaka, Nature **355**, 426 (355); C. Schmidt, K. Svodoba, N. Lei, I. Petsche, L. Berman, C. Safinya, and G. Grest, Science **259**, 952 (1993).
[3] M. Plischke and D.H. Boal, Phys. Rev. A **38**, 4943 (1988).
[4] D.H. Boal, E. Levinson, D. Liu, and M. Plischke, Phys. Rev. A **40**, 3292 (1989).
[5] F.F. Abraham, W.E. Rudge, and M. Plischke, Phys. Rev. Lett. **62**, 1757 (1989); J.-S. Ho and A. Baumgärtner, *ibid.* **63**, 1324 (1989).
[6] F.F. Abraham and D.R. Nelson, J. Phys. (Paris) **51**, 2653 (1990); Science **249**, 393 (1990).
[7] G. Grest and M. Murat, J. Phys. (Paris) **51**, 1415 (1990).
[8] M. Plischke and B. Fourcade, Phys. Rev. A **43**, 2056 (1991).
[9] M. Goulian, J. Phys. II France **1**, 1327 (1991).
[10] P. Le Doussal, J. Phys. A **25**, L469 (1992).
[11] E. Guitter and J. Palmeri, Phys. Rev. A **45**, 734 (1992).
[12] P. Le Doussal and L. Radzihovsky, Phys. Rev. Lett. **69**, 1209 (1992).
[13] G. Grest, J. Phys. I France **1**, 1695 (1991).
[14] Y. Kantor and D. R. Nelson, Phys. Rev. Lett. **58**, 2774 (1987).
[15] Y. Kantor and K. Kremer, Phys. Rev. E **48**, 2490 (1993).
[16] S.J. Barsky, D.H. Boal, and M. Plischke (unpublished).
[17] This criterion, by itself, clearly cannot distinguish a flat phase from a nontrivial crumpled phase with $R_g \sim L^{\nu}$. However, at $\sigma_c(n)$, as defined in the text, the effective exponents $\nu_{3,4}$ are substantially larger than $\nu_{1,2}$ and we therefore assume that $\sigma_c(n)$ is the dividing point between phantom and flat phases.